Theoretical Analysis of Thermal Conduction Effect on Frequency Response of a Perturbed Vaporizing Spherical Droplet

Kwassi Anani, Roger Prud'Homme

Flow, Turbulence Combust manuscript No.
(will be inserted by the editor)

Theoretical Analysis of Thermal Conduction Effect on Frequency Response of A Perturbed Vaporizing Spherical Droplet

Kwassi Anani · **Roger Prud'homme**

Received: date / Accepted: date

Abstract In this work, model results of the effect of thermal conduction on frequency response of a perturbed vaporizing spherical droplet are presented and discussed. The linear analysis of dynamic response to small acoustics oscillations are performed on the basis of the Rayleigh criterion for a mean spherical droplet representing the spray of repetitively injected droplets in the combustion chamber. Curves related to different heat exchange coefficients are presented for the frequency response of the vaporization rate. The not-yet-solved case of imposed temperature at the centre of the spherical droplet (isothermal centre regime or isothermal injection regime) is taking into account here. The case is now compared to the case where the feeding process at the centre of the spherical droplet is assumed adiabatic (adiabatic centre regime or adiabatic injection regime). Each feeding case here considered represents a specific boundary condition controlling the whole injection process. The temperature field perturbation inside the droplet is then examined. Comparisons are also made between the adiabatic and the isothermal injection regimes and differences are analysed. It is shown that the characteristic times of the evaporation process, the period of the harmonic perturbation and a particular parameter depending on fuel physical properties do intervene strongly in the behaviour of the vaporizing droplet. Especially, in the isothermal injection regime, due to this particular parameter, high and non-linear frequency responses may appear in the process. The results of this theoretical study may be applied in establishments of combustion systems stability limits.

K. Anani
Laboratory of Renewable Energies, UNESCO Chair, Faculty of Sciences, Université de Lomé, BP 1515, Lomé, Togo
Tel.: (+228) 22 25 50 94
Fax: (+228) 22 21 85 95
E-mail: ananikwassi@yahoo.fr
Ecole Nationale Supérieure d'Ingénieurs (ENSI), Université de Lomé, BP 1515, Lomé, Togo
Tel.: (+228) 22 25 66 42
Fax: (+228) 22 25 97 36

R. Prud'homme
Institut Jean-Le-Rond-d'Alembert, UPMC/CNRS UMR 7190, case 162, 4, place Jussieu, 75252 Paris cedex 05, France

Keywords mean evaporating droplet · isothermal injection regime · harmonic oscillations · response factor · temperature field perturbation

1 Introduction

Combustion instabilities occur in all types of propulsion systems. In liquid rockets engines for instance, the types of problems encountered since their invention still persist. This is the case of high-frequency transverse modes resulting from a coupling between the combustion processes and the chamber acoustics. Similarly, although earlier liquid-fueled ramjets had instabilities mainly in the high-frequency range, more compact designs in die late 1970s led to longitudinal oscillations having lower frequencies in the range of a few hundred hertz [1]. The instability term here indicates a phenomenon of interaction between the fluctuation of the release of heat or mass and the acoustic fluctuation. It then results from the coupling between these two phenomena, a self-sustained oscillation. The fluctuations in pressure in a combustion chamber will cause fluctuations of release of heat and mass which generate in their turn higher fluctuations in pressure. The loop once established, instability of release of heat and mass occurs. Those problems received a great deal of attention during the last decades and many papers have been published among which we can cite Bhatia and Sirignano [2], Delplanque and Sirignano [3], Yang and Anderson [4], DiCicco and Buckmaster [5], Dubois et al. [6], Duvvur et al. [7], Harrje and Reardon [8], Heidmann and Wieber [9], Heidmann [10], Prud'homme [11, 12], Prud'homme et al. [13], Anani et al. [14].

On another side, pollution having become an environmental and economic major stake, the reduction of the emissions of polluting gases from engines (planes, cars, industrial furnaces...) has become one of the greatest concerns of researchers in engines. One of the technologies used for the reduction of these emissions is mixtures with low concentration. However, the poor characteristic of these mixtures causes appearance of combustion instability which can cause significant damage to the structure of these machines. In fact, the use of this sort of mixtures of limited flammability causes a succession of extinctions and lightings leading to an acoustic resonance. To perform combustion chambers with low pollutant emission level for instance, the major obstacle remains the acoustics-combustion coupling due to the flammability limit of fuels. Instability appearance due to acoustics fluctuation is an event whose prediction is one of the major concerns of industrialists. It is therefore essential to understand the mechanisms of combustion instabilities to be able to control them.

The dynamic response of a vaporizing droplet to these pressure oscillations is typically computed by using drop-evaporation theory [15–17], on the basis of the Rayleigh criterion [18], with simplifying assumptions [9–14]. The classical model of a continuously fed spherical droplet submitted to acoustics oscillations was first formulated in 1960s by Heidmann ([9] and references therein). In the Heidmann analogy, a spherical droplet of constant volume represents a mean droplet at a fixed place in a combustion chamber, in the steady regime. More precisely, the system frequency response of the spray of repetitively injected drops in the combustion chamber is obtained by considering a mean evaporating droplet at rest, continuously fed at a stationary flow rate. This evaporating droplet represents a mean droplet with constant volume, at a specified location in the combustion chamber, and is supposed to summarize the frequency response of individual drops in the spray. The droplet is assumed to be fed by fuel at a constant average temperature with a constant injection rate. With the simplification of Heidmann and Wieber [9], an infinite thermal diffusivity of the liquid is considered; therefore the mean droplet has a uniform temperature.

In the analysis of Prud'homme et al. [13], a finite thermal diffusivity of the liquid is taken into account. The feeding comes from a point source placed at the mean droplet centre. A linear analysis of small harmonic perturbations in which evaporating mass response factor is considered was performed under simplifying assumptions. The latter are zero temperature gradient in the centre of the droplet (adiabatic condition) and neglected convection effect in the energy conservation equation for the liquid-phase. Also in this study, a numerical analysis of heat transfer inside the mean evaporating droplet, termed the *multi-layer model*, was reported. In their recent work, Anani et al. [14] replace the spherical droplet by a cylindrical pastille with an impermeable and adiabatic lateral surface. This latter model, also based on the linear analysis of small harmonic perturbations in pressure, enables the analytical study of the response of the mass and the heat of the pastille-shaped droplet under quite all other assumptions. Analytical expressions were derived for response factors and temperature field perturbations inside the pastille-shaped droplet for both isothermal and adiabatic feeding regimes. Namely this analysis has extended the results from [13] to the case where imposed temperature at the feeding point (isothermal condition) and heat convective flow effect were considered during the process.

This paper, in the light of the forgoing examples of theoretical studies, aims at contributing to the linear analysis of low harmonic instability mechanisms in engines by analytical approaches. We come back to the model of the mean spherical droplet with a finite thermal diffusivity, continuously fed at a stationary flow rate in its centre [13]. We also neglect the radial thermal convection effect in the energy conservation equation for the liquid-phase, since we consider a source only concentrated at the droplet centre. But the not-yet-solved case of imposed temperature in the centre of the spherical droplet (isothermal condition assumption) is taken into account. Moreover analytical expressions of temperature field perturbation within the liquid-phase are derived for both isothermal and adiabatic feeding regimes in this new model. As in [11, 13, 14] we will look for the response factor defined as the ratio of evaporating mass or heat flow rate perturbation to the pressure perturbation. First, a frequency response of the vaporization process to small oscillations in pressure will be evaluated for the isothermal and adiabatic centre regimes. Variations in the response factor curves with frequency and thermal exchange coefficient of the vaporization process will be presented for both regimes. In the isothermal feeding regime, parameters depending on fluid physical properties are shown as impacting on the magnitude of the peaks of response factor curves. Finally, a specific analysis of temperature field perturbation will be performed. It is shown that, in some concrete cases, significant differences appear for the perturbation propagation between the isothermal and the adiabatic feeding regimes. Some of the results have been compared with those of models that accounted for the actual changing volume due to vaporization of individual injected droplets.

2 Formulation of the model

In a physical model, the fuel is injected into the combustion chambers in the form of droplets with a certain mass flow rate. After the atomization processes, some of these transient droplets, depending on their final size reach a stabilized state and are then vaporized. The resulting fuel vapour is burned in contact with gas oxidant. The book of Prud'homme [11] details the generally adopted assumptions for the situation in which fuel injected droplets reach this stabilized state corresponding to a state of rest in an infinite atmosphere. Note that in all this study, all primed quantities denote perturbation quantities (i.e. $x' = (x - \bar{x})/\bar{x}$) whereas all barred quantities denote mean values corresponding to the stabilized state.

2.1 General assumptions

After injection, a transient evaporating droplet generally needs a certain relaxation time to reach a stabilized state. This state is characterized by: constant evaporation rate $\overline{\dot{M}}$, uniform temperature $\overline{T}_S$ of saturated vapour at the droplet surface, and equal velocities of ambient gas and the droplet. Even for stabilized droplets, acoustic waves generated by the engine may cause departure from the stabilized state. The acoustic oscillations normally affect the vaporizing droplet acceleration as well as heat and mass transfer processes by giving the droplet three-dimensional velocity components and causing perturbations within the droplet temperature and its evaporation rate. But Heidmann and Wieber's numerical evaluation of the perturbation curves in vaporization rate [10] showed that the velocity difference contribution to the vaporization rate at high and low pressure were nearly equal and thus cancelled effects with regard to response factor evaluations. As an approximation, therefore, the velocity difference effects on vaporization rate were ignored. Taking on that hypothesis, we also consider in this paper the case of a velocity-stabilized spherical droplet. To study the instabilities generated or amplified by evaporation of a spray of repetitively injected drops in the combustion chamber, we now suppose a mean evaporating spherical droplet, with constant average radius $\overline{r}_S$, located at a velocity node but at a pressure anti-node within a hot gaseous environment of infinite extent.

The mean evaporating droplet is continuously fed on the same incompressible fluid at its centre by a steady flow rate. The density, the specific heat and the thermal conductivity of the droplet are respectively denoted by ρ_L, c_L and k_L. We assume that these thermal properties remain spatially and temporally constant in the droplet during the process. The evaporating droplet is continuously fed by the same fluid with the average mass flow rate $\overline{\dot{M}}$ while using a point source located at the centre of the droplet and in such a way that the spherical symmetry of the droplet is assured at every moment. The feeding of the spherical droplet by the same fluid at the constant density ρ_L is realised at a rate $\overline{\dot{M}}$ in such a way that thermal dilatation of the liquid phase is negligible. In order to neglect also the radial thermal convection inside the continuously fed droplet from its centre to its evaporation surface, we will assume that the local feeding rate $\overline{\dot{M}}$ is not distributed through the droplet.The introduction of a distributed feeding rate into the droplet is not essential if we consider the case of that source only concentrated at the centre as shown in Fig. 1a. Let us note that distributions of singularities of flow or vortex are frequently used for calculations in ballistics. During the injection, the centre of the droplet is assumed to be adiabatic (zero temperature gradient) or isothermal (imposed constant temperature).

The gas-phase includes a diffusion flame model in the gas film surrounding the droplet as we suppose that injected fuel and oxidizer enter separately into the combustion chamber. We will also be concerned only with vaporization dynamics. The influence of combustion will be limited to imposing a stationary composition and temperature at infinity. The combined effects of vaporization dynamics and combustion kinetics, and their eventual retro-action on ambient pressure will not be analyzed here. The droplet is assumed to be vaporizing in combustion gases, composed of stoichiometric reaction products. We will assume that the gas-phase is in the quasi-steady regime as in [15–17]. Consequently the derived perturbation equations established for the gas-phase of the evaporating droplet in [13] are appropriate for this spherical droplet model and will be used. Far from the droplet, the gaseous environment is at constant temperature T_C and at constant pressure P_C. The system pressure is much less than the critical pressure of the liquid, and therefore critical phenomena are not important. Radiation and second-order effects such as Soret and Dufour effects are assumed to

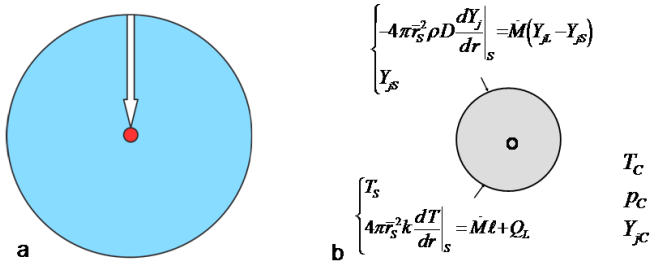

Fig. 1 **a** The mean vaporizing droplet, continuously fed by a source concentrated at its centre. **b** Boundary conditions of a vaporizing droplet. Parameters ρ, D and k denote respectively the density, the mass diffusion coefficient and the thermal conductivity of the gas-phase. The subscripts S and C refer respectively to the conditions at the droplet surface and infinity (i.e. the combustion chamber) and Y_j designates the mass fraction of jth species

be negligible. Convective transport and recirculation within the droplet are neglected and, as mentioned in the introduction, equilibrium conditions at the droplet/gas interface are assumed. The boundary conditions of vaporizing droplet are shown in Fig. 2b. Subscripts L and l refer to liquid-phase whereas subscript S refers to the conditions at the droplet surface.

2.2 Characteristic times

The characteristic times of the vaporization process are the residence time of the droplet and the transfer time by thermal diffusion process. The residence time of the mean droplet, which corresponds to the residence time of the injected liquid for the droplet, replaces the notion of the free droplet lifetime in the present situation of constant volume. The mean residence time $\overline{\tau}_v$ is then written $\overline{M}/\overline{\dot{M}}$ where M is the mass of the supplied droplet and $\overline{M}$ its mean value. The transfer time by thermal diffusion process is $\overline{\tau}_T = \overline{r}_S^2/\kappa_L$ (where $\kappa_L = k_L/\rho_L c_L$ is the thermal diffusivity of the liquid). Thus we defined the thermal exchanged coefficient of the vaporization process as the timescale ratio $\theta = 9\overline{\tau}_v/\overline{\tau}_T = \overline{\tau}_v/\tilde{\tau}_T$ (the coefficient 9 permits to obtain later a simple expression of the transfer function). It has been shown in previous studies [19, 20] that in liquid rocket engines, the acoustic periods of the chamber modes (about 10^{-4} to 10^{-3} s) may be of the same order of magnitude as the characteristic times of vaporization and combustion, whereas the primary and secondary atomization phenomena intervene at smaller time scales. The total mass balance of the droplet is:

$$\frac{\mathrm{d}M}{\mathrm{d}t} = \overline{\dot{M}} - \dot{M} \tag{1}$$

where $\overline{\dot{M}}$ is the stationary flow of injection and $\dot{M}$ the instantaneous flow of evaporation of the droplet. In a stabilized regime, one has: $\overline{\dot{M}} \equiv \dot{M}$, $\mathrm{d}M/\mathrm{d}t = 0$ and $M = \overline{M}$.

2.3 Energy equations

The distribution of the temperature inside the mean evaporating droplet closely depends on the feeding process at its centre and on the thermal conductivity of the fluid. In our present

model with negligible radial thermal convection inside the continuously fed droplet, we rather consider a point source only concentrated at the centre of the droplet. In the presence of such a concentrated flow at the droplet centre, the local mass feeding rate Ω is not distributed within the droplet and we set $\Omega(r) = \overline{\dot{M}}\delta_0(r)$ where δ_0 is a specific delta function which is defined by the relationships as follows:

$$\begin{cases} \delta_0(0) = 1 \\ \delta_0(r) = 0,\ 0 < r \leq \bar{r}_S \end{cases} \tag{2}$$

The centre of the droplet ($r = 0$) must be considered as a singular point since all the injected liquid mass $\overline{\dot{M}}$ is concentrated at this point. In actual fact, one can admit that δ_0 is a function which is almost zero for all values of r except in an infinitesimally small region in the neighbourhood of the point $r = 0$ where it takes the unity value.

The radial thermal convection effect can then be neglected and only pure thermal conduction effect is taken into account. In these conditions, $T_l \equiv T_l(r,t)$ being the time-temperature function value at the radial coordinate r in the liquid phase, the energy equation within the droplet is written:

$$\rho_L c_L \frac{\partial T_l}{\partial t} - \frac{k_L}{r}\frac{\partial^2 (rT_l)}{\partial r^2} = 0 \tag{3}$$

subject to $\left.\frac{\partial T_l}{\partial r}\right|_{0,t} = 0$, $T_l(\bar{r}_S,t) = T_S(t)$ for the adiabatic injection at the centre or to $T_l(0,t) = \overline{T}_S(t)$, $T_l(\bar{r}_S,t) = T_S(t)$ for the isothermal injection at the droplet centre. The heat Q_L transferred into the droplet is given by:

$$4\pi \bar{r}_S^2 k_L \left.\frac{\partial T_l}{\partial r}\right|_{\bar{r}_S,t} = Q_L = Q - \dot{M}\ell \tag{4}$$

where Q_L and ℓ are respectively the external gas heat flux and the latent heat of vaporization per unit mass of the liquid. This condition couples the gas and the liquid-phase solutions at the spherical droplet surface.

3 Linear analysis for small perturbations

The advantage of the linear analysis for subcritical vaporization models is that it provides dimensionless parameters related to fuel properties that may be used to characterize and examine the dynamic behaviour of the vaporization process for any fuel.

3.1 The linearized equations

Assuming that the supplied spherical droplet has reached a stabilized state, we now consider small acoustic perturbations writing $f = \bar{f} + \Delta f$ where f is a flow parameter, $\bar{f}$ is its mean value, Δf is the corresponding absolute perturbation, and $f' = \Delta f/\bar{f}$ is the corresponding relative perturbation. The equation of energy conservation can be written:

$$\rho_L c_L \frac{\partial T_l'}{\partial t} - \frac{k_L}{r}\frac{\partial^2 (rT_l')}{\partial r^2} = 0 \tag{5}$$

and the flow at the surface is given by:

$$4\pi\bar{r}_S^2 k_L \overline{T}_S \left.\frac{\partial T_l'}{\partial r}\right|_{\bar{r}_S,t} = \Delta Q_L \tag{6}$$

The boundary conditions in the adiabatic feeding regime are:

$$\begin{cases} \left.\dfrac{\partial T_l'}{\partial r}\right|_{0,t} = 0 \\ T_l'(\bar{r}_S,t) = T_S'(t) \end{cases} \tag{7}$$

and become in the isothermal feeding regime:

$$\begin{cases} T_l'(0,t) = \overline{T}_S' = 0 \\ T_l'(\bar{r}_S,t) = T_S'(t) \end{cases} \tag{8}$$

3.2 Analytical solutions

Introducing small harmonic perturbations of pulsation ω i.e. of the form $f' = \hat{f}(r)\mathrm{e}^{i\omega t}$, we set $T_l' = \hat{T}_l(r)\mathrm{e}^{i\omega t}$ and $\Delta Q_L = \Delta\hat{Q}_L(r)\mathrm{e}^{i\omega t}$.

In the adiabatic centre case one can find a solution $\hat{T}_l$, continuous at $r = 0$, which takes the form: $r\hat{T}_l = C_1(\mathrm{e}^{s_0 r} - \mathrm{e}^{-s_0 r})$ while in the isothermal feeding case a solution can be expressed in the form: $r\hat{T}_l = C_2(\delta_0(r) - \cos(\bar{s}_0 r))$ with C_1 and C_2 being constant, δ_0 the delta function defined by relations 2, $s_0 = (1+i)\sqrt{\omega/(2\kappa_L)}$ and $\bar{s}_0 = (1-i)\sqrt{\omega/(2\kappa_L)}$ two conjugate complex numbers. Note that s_0 and $-s_0$ are the two complex roots of the characteristic equation $i\omega - \kappa_L s^2 = 0$ obtained from Eq. 5. Using respectively conditions 7 and 8 at the droplet surface, one has $C_1 = \hat{T}_S\bar{r}_S/(\mathrm{e}^{s_0\bar{r}_S} - \mathrm{e}^{-s_0\bar{r}_S})$ for the adiabatic feeding case and $C_2 = -\hat{T}_S\bar{r}_S/\cos(\bar{s}_0\bar{r}_S)$ for the isothermal feeding case. The expression of the solution for the temperature field in the droplet for the adiabatic regime now reads:

$$r\hat{T}_l = \frac{\bar{r}_S\hat{T}_S\,(e^{s_0\,r} - e^{-s_0\,r})}{e^{s_0\,\bar{r}_S} - e^{-s_0\,\bar{r}_S}} \tag{9}$$

while in the isothermal regime one has:

$$r\hat{T}_l = -\frac{\bar{r}_S\,\hat{T}_S\,(\delta_0\,(r) - \cos\,(\bar{s}_0 r))}{\cos\,(\bar{s}_0\bar{r}_S)} \tag{10}$$

We may notice that the boundary conditions of the isothermal centre regime are well verified by the last solution (Eq. 10) which is continuous with regard to r in $[0,\bar{r}_S]$ except at $r = 0$.

Let us introduce the reduced frequency $u = 3\omega\overline{\tau}_v$. The flow condition at the droplet surface $4\pi\bar{r}_S^2 k_L\overline{T}_S \left.\frac{\mathrm{d}\hat{T}_l}{\mathrm{d}r}\right|_{\bar{r}_S} = \Delta\hat{Q}_L$ applies to equations 9 and 10. That leads to:

$$\Delta\hat{Q}_L = -4\pi\bar{r}_S k_L\overline{T}_S E(u,\theta)\hat{T}_S \tag{11}$$

where E is a function of u and θ. For the adiabatic feeding case, one has $E = 1 - s_0\bar{r}_S\coth(s_0\bar{r}_S)$ whereas for the isothermal feeding case the calculation yields $E = 1 + \bar{s}_0\bar{r}_S\tan(\bar{s}_0\bar{r}_S)$ with $s_0\bar{r}_S = (1+i)\sqrt{3u/2\theta}$, $\bar{s}_0\bar{r}_S = (1-i)\sqrt{3u/2\theta}$ and $\theta = 9\kappa_L\overline{\tau}_v/\bar{r}_S^2 = \overline{\tau}_v/\tilde{\tau}_T$.

3.3 The transfer function

The linearized equations for the liquid/gas interface [13,14,21], based on the classical theory of quasi-stationary spherical drop [16,17] will now be used. The unperturbed state is a stable situation for which any thermodynamic variable f of droplet has a uniform distribution $\bar{f}$. For small harmonic disturbances, we set $\Delta f = f - \bar{f}$, $f' = \Delta f/\bar{f}$ and $f' = \hat{f}(r)\mathrm{e}^{i\omega t}$. The ambient pressure is given by $p' = \hat{p}_C\,\mathrm{e}^{i\omega t}$. From the study of the gas phase [13] it was deduced that:

$$\hat{M} = \alpha \frac{iu}{1+iu}\left(\overline{b}\hat{T}_S - \hat{p}_C\right) \tag{12}$$

with $u = 3\omega\overline{\tau}_v$, $\dot{M}' = \Delta\dot{M}/\overline{\dot{M}} = \hat{\dot{M}}\mathrm{e}^{i\omega t}$ and:

$$\Delta\hat{Q}_L = \overline{\dot{M}}\overline{\ell}\left(\overline{a}\hat{p}_C - \mu\hat{T}_S\right) \tag{13}$$

where $\Delta Q_L = Q_L - \overline{Q}_L = Q_L = \Delta\hat{Q}_L\mathrm{e}^{i\omega t}$ as $\overline{Q}_L = 0$.

In these equations we recalled that $\dot{M}$, Q_L, T_S, p_C and ℓ are respectively the mass flow rate of evaporation, the heat flow penetrating into the drop from the surrounding gas mixture, the surface temperature, the pressure chamber and the latent heat of evaporation. The coefficients used in these equations are:

$$\begin{cases} \overline{a} \;=\; \dfrac{\overline{T}_C}{\overline{T}_C - \overline{T}_S}\,\dfrac{\gamma-1}{\gamma} + \varphi, \quad \overline{b} = \dfrac{\overline{T}_S}{\left(\overline{T}_S - c\right)^2}\,b, \quad \mu \;=\; \dfrac{\overline{T}_S}{\overline{T}_C - \overline{T}_S} - \dfrac{2c}{\overline{T}_S - c} + \overline{b}\varphi \\ \\ \alpha \;=\; \dfrac{\overline{B}_M}{\left(1+\overline{B}_M\right)\,\ln\left(1+\overline{B}_M\right)}\,\dfrac{\overline{Y}_{AC}\overline{Y}_{FS}}{\overline{Y}_{AS}\left(\overline{Y}_{FS} - \overline{Y}_{FC}\right)}\,\dfrac{\mathrm{M}_F}{\mathrm{M}_F\overline{X}_{FS} + \mathrm{M}_A\overline{X}_{AS}} \end{cases}$$

In these definitions F designates the fuel, A represents the burnt gases, C the chamber and S the surface of the drop, the quantities Y_j, B_M, M_j, γ are respectively the mass fraction of species j, the Spalding parameter for the mass, the molecular weight of species j and the isentropic coefficient (assumed to be constant). The coefficients b and c are derived from the expression of the latent heat given in the form: $\ell = bRT_S^2/\mathrm{M}_F\,(T_S - c)^2$. The function φ corresponds to the quantity $\varphi = \overline{Y}_{AC}\overline{Y}_{FS}\mathrm{M}_F\,/\,\overline{Y}_{AS}(\overline{Y}_{FS} - \overline{Y}_{FC})(\mathrm{M}_F\,\overline{X}_{FS} + \mathrm{M}_A\,\overline{X}_{AS})$.

Eliminating $\Delta\hat{Q}_L$ in 13 and 11 and using 12, the expression for the complex transfer function $Z = \hat{M}/(\alpha\hat{p}_C)$ is obtained:

$$Z = \frac{iu}{(1+iu)}\,\frac{A + \theta E(u,\theta)}{B - \theta E(u,\theta)} \tag{14}$$

with $A = 3\left(\overline{a}\overline{b} - \mu\right)/\lambda$ and $B = 3\mu/\lambda$ ($\lambda = c_L\overline{T}_S/\overline{\ell}$). One can see that the parameters A and B are thermodynamic coefficients related to the fuel physical properties.

4 Response factor

A response factor can be defined as being one measure of the magnitude by which the evaporation process can reinforce an acoustic oscillation. This response factor is based on the Rayleigh criterion for acoustic amplification by heat or mass addition. This criterion states that reinforcement or amplification occurs when an excess of heat or mass is added while the pressure is greater than the mean value.

4.1 The reduced response factor

The reduced pressure perturbation is defined as $p' = (p - \bar{p})/\bar{p}$, and the resulting reduced heat or mass perturbation is $q' = (q - \bar{q})/\bar{q}$. The response factor N is defined as:

$$N = \frac{\iint\limits_{V,t} q'(V,t)\, p'(V,t)\, \mathrm{d}t\mathrm{d}V}{\iint\limits_{V,t} (p'(V,t))^2\, \mathrm{d}t\mathrm{d}V} \tag{15}$$

where the double integral value is calculated over a given period of time t in a finite volume V. For sinusoidal oscillations which are uniform over a finite volume, one has $N = (|\hat{q}|/|\hat{p}|)\cos\phi$, where $|\hat{q}|$, $|\hat{p}|$ are the moduli and ϕ is the phase difference between q' and p'. The response factor N is expressed as the ratio of the magnitude of heat or mass perturbation to the magnitude of the pressure perturbation and thus, includes phase relations. In the rest of this paper we will consider and call response factor, the reduced response factor, which is the real part of the transfer function Z [13, 14]:

$$\frac{N}{\alpha} = \Re(Z) \tag{16}$$

The response factor is assumed positive when the vaporization rate and the chamber pressure are either above or below their mean values and assumed negative when the vaporization rate and the chamber pressure are on the opposite sides of their means. Following the well-known Rayleigh criterion [18], an unsteady evaporation and burning can be one possible driving mechanism of instability [4, 8].

4.2 Results and discussions

The treatment of the data consists to relate the response factor to the characteristic times of the processes involved. As mentioned in Sect. 2.2, these times are the residence time of the droplet and the transfer time by thermal diffusion process. Variations in response factor curves with reduced frequency u are shown for arbitrary values of the exchange coefficient $\theta = \overline{\tau}_v/\tilde{\tau}_T$ (ratio of the characteristic times of the process). All the presented curves have been obtained with $A = 10$ and $B = 100$. These values of A and B have being used in precedent articles [13, 14], for they correspond to orders of magnitude of values encountered in the classical fuels. In each diagram of Fig. 2, different response factor curves corresponding to particular values of parameter θ are presented.

In the adiabatic centre regime, the response factor shows always a positive response region. It exhibits a peak value around a fixed reduced frequency value u_p nearly equals to 3. A typical response factor curve approaches zero at a lower frequency and decreases to negative values at higher frequencies. The cut-off reduced frequency u_c for a zero response factor, therefore, divides the frequency response into regions of destabilizing and stabilizing influences, and may be considered as a critical frequency. When θ increases from 1 on, the critical frequency u_c tends to decrease quickly first, reaches a minimum value for θ about 10 and then begins to increase very slowly and tends to attain a limit frequency value slightly greater than 30 (Figs. 2c and 2e). Indeed in this regime, it was found [14] that when $\theta \to \infty$, critical frequencies or cut-off values tend to a constant value equal to $\sqrt{A + AB + B}$ ($\cong 33.3$ for $A = 10$ and $B = 100$). We also notice concerning the peak value that it increases slightly with θ and tends to a value about 0.1 as shown in Figs. 2c and 2e.

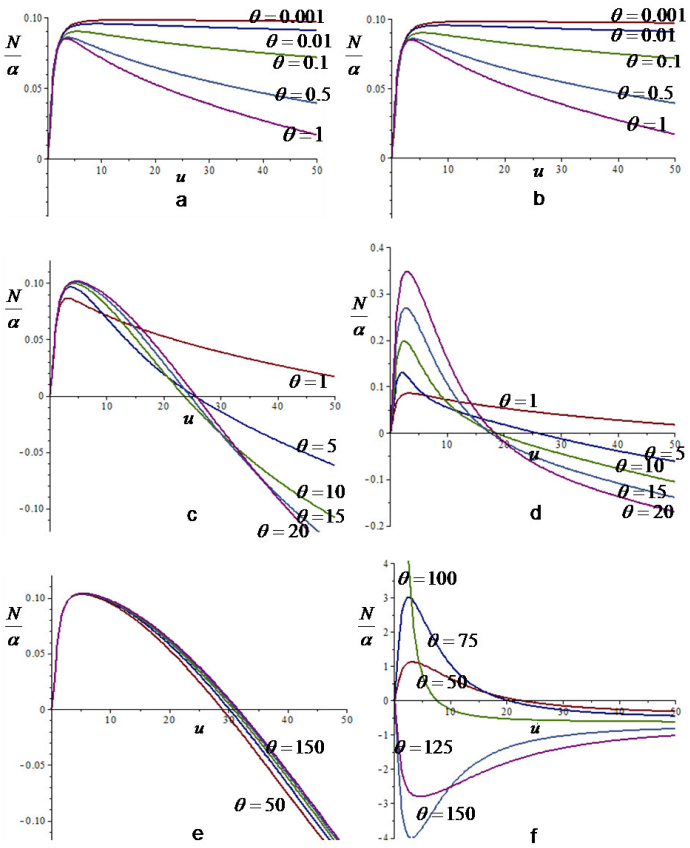

Fig. 2 Influence of reduced exchange coefficient θ on the response factor for the mean spherical droplet with $A = 10$ and $B = 100$. **a** Adiabatic centre. **b** Isothermal centre. **c** Adiabatic centre. **d** Isothermal centre. **e** Adiabatic centre. **f** Isothermal centre

On the other side, in the isothermal centre regime, the critical frequency u_c if it exists, turns about 20 when $10 < \theta \leq 75$ (Fig. 2d) but decreases significantly until about 7 when $\theta = 100$ (Fig. 2f) whereas the peak value, always at about the same frequency $u_p \cong 3$ as for adiabatic injection regime, grows very quickly and seems to tend to infinity for this value of $\theta = 100$. In fact, larger peak values appear for $1 < \theta \leq 50$ and grow very quickly beyond the unity value for $50 < \theta < 100$. For these values of θ , the isothermal injection regime apparently introduces nonlinearity in the vaporization process that increases significantly the peak value of response factor at this specific frequency u_p. Especially, for $\theta = 100$ the frequency response curve for isothermal feeding regime asymptotically diverges from unity to infinity, along the vertical line passing at u_p. But curves for higher values of θ ($\theta > 100$) show negative response factors for all frequencies.

For both adiabatic and isothermal feeding regimes, the frequency response curves are quite similar for relatively small values of the exchange coefficient ($0 < \theta \leq 1$) as shown in Figs. 2a and 2b. Likewise, for both regimes, the peak responses seem to be at a same specific frequency u_p, which is relatively unaffected by the variations of θ. To the contrary, the cut-off frequency u_c, if it exists in the isothermal centre regime, is noticeably lower than that of

the adiabatic centre regime for the same value of the characteristic times ratio θ. The main differences in the frequency response for the isothermal injection regime compared with the adiabatic one are the larger peak values of the response factor at the particular frequency u_p and the absence of a positive response region when $\theta > 100$.

4.3 Analysis of results

In frequency limit cases, the reduced response factor N/α tends to the same value in both adiabatic and isothermal centre regimes. In effect, in the low frequency limit $u \to 0$, $N/\alpha \to 0$ and in the high frequency limit $u \to \infty$, $N/\alpha \to -1$. A response factor of less than zero will always signify that the evaporation mechanism has a stabilizing influence upon the system, whereas a positive response has rather a driving influence by tending to reinforce the instability.

As already shown for the pastille-shaped droplet model in [14], we notice here too that for both adiabatic and isothermal centre regimes, the peak value of the response factor occurs at the same reduced frequency $u_p \cong 3$. But $u_p \cong 3$, that is $\omega\overline{\tau}_v \cong 1$, means that the response factor is at the maximum when the droplet lifetime (injected liquid residence time $\overline{\tau}_v$) is at the same order of magnitude as the oscillation period. As the droplet residence time approaches the period of the oscillation, the droplet mass transfer flow rate by evaporation mechanism can respond to the acoustic oscillations. This favours mass transfer in phase with pressure, and results in a peak positive response factor.

The reduced frequency $u_p \cong 3$ is relatively low, and in the neighbourhood of such a low frequency, assuming that the characteristic times ratio θ is sufficiently large, the ratio $x = u/\theta$ can be supposed negligible in the expression of the complex transfer function Z (Eq. 14). Thus, an estimation of Z obtained by a limited expansion according to $x = 0$ (while assuming u closer to u_p) gives for the adiabatic centre regime the expression:

$$Z \cong \frac{iuA}{(1+iu)B} \tag{17}$$

whereas in the isothermal centre case we obtain:

$$Z \cong \frac{iu(A+\theta)}{(1+iu)(B-\theta)} \tag{18}$$

The latter relation furnishes the explanation for the response factor significant deviations from the unity value to infinity, around the particular frequency u_p, for a specific value of θ when being in the isothermal injection regime. Indeed, in the isothermal centre regime, when the ratio θ amounts to B while remaining lower than it, the response factor which is nearly the real part of the estimated expression of Z (Eq. 18), tends to infinity at the peak-value reduced frequency u_p. Once θ is taken greater than B the reduced response factor curve is turned upside down along the horizontal line $N/\alpha = -1$ and shows only negative response factors for all frequencies. Since $B = 3\mu/\lambda$ is related to the fuel properties (heat capacity, latent heat, surface temperature, saturated pressure at surface), it appears that in the isothermal centre regime, fuel properties can influence strongly the instability phenomenon for ratio θ tending to B. These response factor deviations around the frequency u_p in this limit case ($\theta \to B$) may indicate eventual break-up phenomena. They could also be one of the possible causes for the appearance of non-linear and high frequency instabilities in the combustion chamber. Anyway, an experimental work is needed to clarify the issue.

It is equally noteworthy that in the low time ratio limit $\theta \to 0$, the above estimated expressions 17 and 18 of the complex transfer functions Z in both regimes are almost identical. Then, the response factor values in both regimes are nearly equal around the reduced frequency u_p corresponding to their peak value. Therefore, in both regimes, the corresponding curves are similar for all frequencies as shown in Figs. 2a and 2b.

Another point we may notice in this analysis is that the residence time $\overline{\tau}_v$ does not intervene in the ratio $x = u/\theta$ but only the thermal diffusion time $\overline{\tau}_T$ and the pulsation of the oscillating wave ω intervene. Therefore taking the ratio $x = u/\theta = \omega\overline{\tau}_T/3$ negligible at the fixed frequency $u_p = 3\omega\overline{\tau}_v \cong 3$ implies taking $\overline{\tau}_T$ negligible with regards to the oscillation period $\Gamma = 2\pi/\omega$. Since $\omega\overline{\tau}_T \ll 1$, that is $\overline{\tau}_T \ll \Gamma$, the two processes that are thermal diffusion and oscillation wave propagation are no more in phase. This is especially apparent when $\theta > B$ for curves in Fig. 2f in which the droplet temperature is held constant, since the feeding process at the centre of the droplet is isothermal. As a result, at the frequency u_p, the response factor falls into a negative peak value less than the standard minimal value of -1, and remains negative for all other frequencies. We can conclude that in the isothermal injection regime, non-linear response factor can occur, especially around the peak-value reduced frequency u_p when θ is taken closer to B.

5 Temperature field perturbation

The temperature profile inside the spherical droplet depends on the frequency of the oscillation, and a temperature perturbation can be evaluated. As the response factor is the frequency response of mass transfer to the acoustic oscillations, the reduced temperature perturbation is the response of the temperature field to the same acoustic forcing.

5.1 The reduced temperature perturbation

The reduced temperature perturbation is defined as [14]:

$$T'_{lred}(u,\theta,\xi,\tau) = \Re\left(\hat{T}_{l\,red}\,\mathrm{e}^{iu\frac{\tau}{3}}\right) \tag{19}$$

for the reduced quantity $\hat{T}_{lred} = \overline{b}\hat{T}_l/\hat{p}_C$ with the reduced radius $\xi = r/\overline{r}_S$ and the reduced time $\tau = t/\overline{\tau}_v$. We deduce from Eqs. 12 and 14 the following relation for the value of $\hat{T}_S$:

$$\hat{T}_S = \frac{\hat{M}}{Z\alpha\overline{b}}\frac{A+\theta E(u,\theta)}{B-\theta E(u,\theta)} + \frac{\hat{p}_C}{\overline{b}} \tag{20}$$

We now set $m = s_0\overline{r}_S$ and $\overline{m} = \bar{s}_0\overline{r}_S$. Taking into account the expression of $\hat{T}_l$ in Eq. 9 and the expression of the transfer function $Z = \hat{M}/(\alpha\hat{p}_C)$, we have for the adiabatic injection regime:

$$\hat{T}_{lred}(u,\theta,\xi) = \frac{A+B}{(B-\theta E(u))}\frac{1}{\xi}\frac{\mathrm{e}^{m\xi}-\mathrm{e}^{-m\xi}}{\mathrm{e}^{m}-\mathrm{e}^{-m}} \tag{21}$$

and

$$T'_{lred}(u,\theta,\xi,\tau) = \Re\left(\frac{A+B}{(B-\theta E(u))}\frac{1}{\xi}\frac{\mathrm{e}^{m\xi}-\mathrm{e}^{-m\xi}}{\mathrm{e}^{m}-\mathrm{e}^{-m}}\,\mathrm{e}^{iu\frac{\tau}{3}}\right) \tag{22}$$

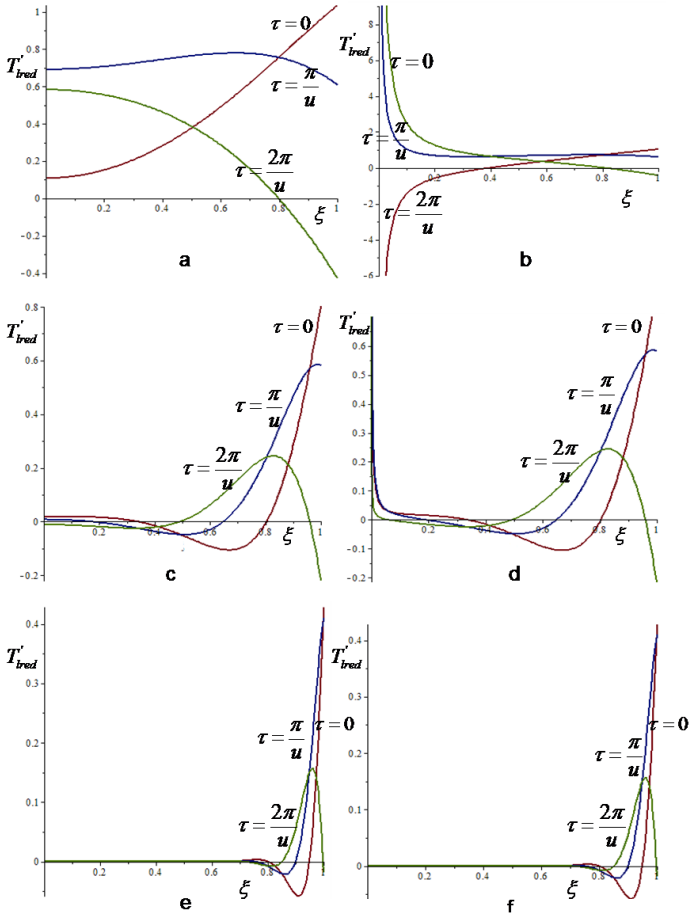

Fig. 3 Reduced temperature perturbation inside the droplet with $A = 10$ and $B = 100$: browsing in time over semi period. **a** Adiabatic centre $\theta = 5$, $u = 15$. **b** Isothermal centre $\theta = 5$, $u = 15$. **c** Adiabatic centre $\theta = 5$, $u = 150$. **d** Isothermal centre $\theta = 5$, $u = 150$. **e** Adiabatic centre $\theta = 5$, $u = 1500$. **f** Isothermal centre $\theta = 5$, $u = 1500$

with the expression of function E corresponding to the adiabatic injection case (see Sect. 3.2). For the isothermal centre regime, the calculations yield:

$$\hat{T}_{lred}(u, \theta, \xi) = \begin{cases} 0, \ \xi = 0 \\ \dfrac{A+B}{(B-\theta E(u))} \dfrac{1}{\xi} \dfrac{\cos(\overline{m}\xi)}{\cos(\overline{m})}, \ \xi > 0 \end{cases} \tag{23}$$

and

$$T'_{lred}(u, \theta, \xi, \tau) = \begin{cases} 0, \ \xi = 0 \\ \Re\left(\dfrac{A+B}{(B-\theta E(u))} \dfrac{1}{\xi} \dfrac{\cos(\overline{m}\xi)}{\cos(\overline{m})} \mathrm{e}^{iu\frac{\tau}{3}} \right), \ \xi > 0 \end{cases} \tag{24}$$

with the expression of function E corresponding to the isothermal injection case (see Sect. 3.2).

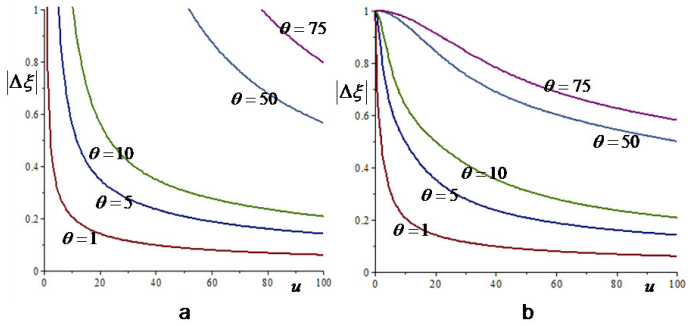

Fig. 4 Thermal wave-penetration depth $|\Delta\xi|$ as function of the reduced frequency u for different values of the exchange coefficient θ. **a** Adiabatic centre. **b** Isothermal centre

5.2 Results and discussions

Plotting the reduced temperature perturbation $T'_{lred}(u,\theta,\xi,\tau) = \Re(\hat{T}_{l\,red}\,e^{iu\frac{\xi}{3}})$ as function of the reduced abscissa ξ is realized through browsing in time over semi-period ($\tau = t/\overline{\tau}_v = 0,\ \pi/u,\ 2\pi/u$) for different values of θ. The cases $\theta = 5$ and $u = 15$; 150; 1500 for both isothermal and adiabatic injection regimes are presented in Fig. 3. All the shown curves have been calculated with $A = 10$ and $B = 100$. The curves in Fig. 3 present the wave penetration depth inside the spherical droplet and the magnitude of the variation of the temperature perturbation amplitude related to varying time τ.

In the isothermal injection regime, due to the discontinuity of the expression of the derived solution (Eq.10) at the centre of the droplet ($r = \xi = 0$), the reduced temperature perturbation diverges from zero at that point for some ranges of the frequency u and the ratio θ. These divergences from zero at $\xi = 0$ as shown in Figs. 3b and 3d for $\theta = 5$ and $u = 15$; 150, are not related to the interpretation of the physical phenomenon but their occurrence or absence may indicate whether the thermal wave has reached the centre of the droplet or not. But for large values of the reduced frequency u with regard to the exchange coefficient θ, it is noticeable that the temperature perturbation amplitude yields the same profile in both regimes as in Figs. 3e and 3f for $\theta = 5$ and $u = 1500$. In the adiabatic centre regime, the reduced temperature perturbation takes its values in the interval $[-1, 1]$. As in the isothermal centre regime, the increase of u at a fixed θ tends to reduce the penetration depth of the perturbation (see Fig. 3). Remarkably, the calculations show that when $\theta = 100$ and $u = 15 \times 10^6$ the penetration depth of the thermal wave in both regimes is nearly zero.

5.3 Analysis of results

First, the thermal wave-penetration depth $|\Delta\xi| = |\Delta r|/\overline{r}_S$ is localized by the abscissa $\xi_l = r_l/\overline{r}_S$ from which the amplitude of the thermal oscillation becomes null. An estimation of $|\Delta\xi|$ can be obtained by a truncated expansion of the reduced temperature $\hat{T}_{lred} = \overline{b}\hat{T}_l/\hat{p}_C$ at the neighbourhood of $r = \overline{r}_S$ i.e. at the neighbourhood of $\xi = 1$. Thus, according to expressions 21 and 23, the truncated expansion of first order of $\hat{T}_{lred}$ near the surface gives for the adiabatic centre regime $\hat{T}_{l\,red} \approx (A+B)\,(1+(m\coth m - 1)\,\Delta\xi)/(B - \theta\,E)$ and for the isothermal centre regime $\hat{T}_{l\,red} \approx (A+B)\,(1-(1+\overline{m}\tan(\overline{m}))\,\Delta\xi)/(B - \theta\,E)$. Therefore for

both regimes, $\hat{T}_{lred} = 0$ implies:

$$|\Delta\xi|(u,\theta) \approx \left|\frac{1}{E(u,\theta)}\right| \tag{25}$$

where $E(u,\theta) = 1 - m\coth(m)$ for adiabatic injection regime and $E(u,\theta) = 1 + \overline{m}\tan(\overline{m})$ for isothermal injection regime with $m = s_0\bar{r}_S$ and $\overline{m} = \bar{s}_0\bar{r}_S$ (see Sect. 3.2). In Fig. 4, some estimations of the thermal wave-penetration depth $|\Delta\xi|$ as functions of the reduced frequency u are presented for certain values of the exchange coefficient θ. The curves in Fig. 4 confirm the fact that, for these values of θ, the thermal wave-penetration depth $|\Delta\xi|$ tends almost asymptotically to its maximal penetration depth value of 1 at the particular reduced frequency $u_p \cong 3$ where the response factor also attains its peak value.

Second, for large values of the ratio $u/\theta = \omega\overline{\tau}_T/3$, the temperature perturbation profile does not depend on the regime at the centre of the droplet but it seems to be identical in both regimes. Indeed, for $u/\theta \gg 1$ that is $\overline{\tau}_T \gg \Gamma$ (Γ is the period of the harmonic pressure perturbation), the thermal diffusion time is much larger compared to the oscillation period, and the two processes that are thermal diffusion and oscillation wave propagation are no more in phase. A situation in which, the thermal oscillation wave penetration inside the droplet is considerably reduced. To the contrary, when $u/\theta \ll 1$, that is $\overline{\tau}_T \ll \Gamma$, the thermal diffusion time is smaller than the period of the harmonic perturbation and the thermal perturbation wave reaches the centre of the supplied droplet after the heat diffusion transfer is realized inside the droplet. This favours the oscillation wave penetration inside the droplet in both regimes, regardless of the boundary condition at the centre of the droplet. We understand that important differences in the thermal wave propagation between the two regimes may occur only when $\overline{\tau}_T \approx \Gamma$ since the boundary conditions relative to the conduction at the centre of the droplet are kept different.

6 A brief comparative analysis

In this section, we aim to briefly compare some results of the present theoretical model with those of certain other combustion instability models. Through the analyses of the latter we can see the actual changing volume due to vaporization of individual injected droplets in an array. The dynamic behaviour of spray vaporization is thus taken as a statistical consequence of the vaporization characteristics of each individual droplet as generally practised in most numerical simulations in such investigations.

6.1 Unsteady spray vaporization models

It is well known that acoustical oscillations in velocity and pressure can significantly influence all the critical processes involved in the combustion chamber of an engine. These processes can range from atomization, vaporization, unsteady mixing to combustion. The processes in turn help set up such complex feedback loops between pressure and heat release oscillations. According to Rayleigh criterion, when these oscillations are sufficiently in phase, a growth of the initial disturbance results often leading up to disastrous proportions. Particularly, concerning unsteady vaporization under acoustic oscillations, the early simplified analyses by Heidmann and Wieber [9, 10] were applied to an array of repetitively injected drops as well as to the continually fed spherical droplet called mean droplet or Heidmann droplet. The main assumption of this simplified model also termed Heidmann model

is that the liquid thermal diffusivity is assumed infinite leading to a uniform liquid temperature in the analyses. To the contrary, the present model of the continually fed spherical droplet which can also be called a finite diffusivity model, assumes a finite thermal diffusivity in the liquid phase and results of Heidmann model concerning the maximum and cut-off values for the response function are derived just as limit cases [13, 14].

Since 1972, Harrje and Reardon [8] identified five vaporization characteristic times: droplet lifetime, liquid thermal diffusion time, liquid thermal inertia, gas phase diffusion time for a locally stagnant gas field, and forced convection gas phase diffusion time. Pressure and velocity oscillations in the gas phase (acoustic perturbations) can influence the vaporization rate of liquid droplets if the period of oscillation corresponds to one of the abovementioned vaporization characteristic times. This important result fully fits our present model for the following two reasons. First, the analyses have shown that the mass response factor attains its peak value when the mean droplet lifetime (injected liquid residence time $\overline{\tau}_v$) is at the same order of magnitude as the oscillation period Γ. Second, concerning the temperature field perturbation within the droplet, we have understood that major differences in the thermal wave propagation between the two injection regimes (adiabatic and isothermal) may occur only when liquid-phase thermal diffusion time $\overline{\tau}_T$ can be approximated to the oscillation period. As for the pastille-shaped droplet [14], we have found in our present model that the ratio u/θ that is $\overline{\tau}_T/\Gamma$ plays an important role in the temperature field perturbation within the droplet.

In 1996, Delplanque and Sirignano [3] studied the dynamic responses of liquid oxygen droplet (LOX) to oscillatory ambient conditions at subcritical and supercritical pressures. Both cases of an isolated droplet and droplets in an array were considered. Based on simplified assumptions, their numerical analyses have shown that the droplet vaporization process can be a driving factor in longitudinal combustion instabilities. Conclusions were then drawn that droplet secondary atomization, which reduces the droplet lifetime, can significantly influence the droplet vaporization response and combustion instability. As in our present study, the peak value of the mass response factor is strongly correlated with the droplet lifetimes.

6.2 Unsteady single droplet vaporization models

Concerning perturbed single droplet vaporisation studies, Duvvur et al. [7] analyzed since 1996 the vaporization behaviour of a single droplet in an oscillating flow field, and concluded that combustion instability can arise in an evaporation-ratecontrolled chamber for certain oscillation frequency ranges and for initial droplet sizes. More Recently (2011), Hsiao et al. [22] conducted a numerical study of the dynamic responses of n-pentane fuel droplets to externally imposed pressure oscillations under both subcritical and supercritical conditions. Results obtained appear to be correlated in terms of droplet diameter, lifetime, and thermo-physical properties, as well as oscillation frequency. It was shown that an abrupt change in the droplet response intervened when the droplet surface reached its critical mixing state and a major factor contributing to this phenomenon was the rapid variations of fluid thermodynamic properties near the critical mixing point. But our present theoretical analysis indicates that an abrupt variation in the mean droplet response can occur at the particular peak frequency u_p even in a subcritical vaporization process. Being in the isothermal injection regime, this abnormal phenomenon can occur provided that a proximity exists between values of the characteristic times ratio $\theta = 9\overline{\tau}_v/\overline{\tau}_T = \overline{\tau}_v/\tilde{\tau}_T$ and the thermodynamic parameter $B = 3\mu/\lambda$.

Liquid oxygen (LOX) droplet vaporization in quiescent hydrogen/water environments

was investigated by Lafon et al. [23] at subcritical pressures in 2008. Based on the latter, pressure-coupled responses of LOX droplet vaporization and combustion in low and high pressures hydrogen environments were recently (2014) investigated by the same authors [24]. For the pure vaporization case of a single LOX droplet evaporating initially in quiescent hydrogen under subcritical pressure, it was found that mass response factor to pressure perturbation is correlated with the instantaneous value of the liquid-phase thermal diffusion time normalized by the oscillation frequency. Concerning the maximum and cut-off values for the response function, distinct behaviours about one order of magnitude have been found between LOX droplet vaporization in hydrogen [24] and n-pentane fuel droplet evaporating in nitrogen [22]. It was concluded in [24] that this phenomenon can be attributed to the disparity in the ratio of the droplet lifetime to liquid thermal-inertial time. This ratio corresponds precisely to the characteristic times ratio θ in our present model, confirming in this way the fact that maximum and cut-off values of the mass response function are related to θ. Moreover our present model indicates that these particular response function values also depend on some thermodynamic parameters $A = 3\left(\overline{a}\overline{b} - \mu\right)/\lambda$ and $B = 3\mu/\lambda$ and on the nature of the injection regime (adiabatic or isothermal).

But in all these single droplet models [7,22,24], hints were not given about the statistical extrapolation of the results concerning a single vaporising droplet response to that of a spray of repetitively injected droplets in a combustion chamber. Nevertheless, based on results of a single perturbed droplet in subcritical vaporization process, the present finite conductivity model of a continually fed spherical droplet may be envisaged as a generalization from the particular behaviour of a single perturbed droplet to that of an unsteady array or spray of repetitively injected drops in a combustion chamber.

6.3 Contribution from the present model

All the above issues have important implications for the study of combustion instabilities in liquid rocket engines as they have concluded that vaporization is one of the key factors to stimulate the combustion instability in liquid rocket engines. As already indicated, the advantage of the present linear analysis for subcritical vaporization models is that it provides dimensionless parameters related to fuel properties that may be used to characterize and examine the dynamic behaviour of the vaporization process for any fuel. Compared to the above studies the main contribution from this finite diffusivity model of a continuously fed spherical droplet resides in the analysis carried out upon the mean droplet temperature field response to harmonic acoustic disturbances. This specific analysis was not covered by the above-mentioned models.

7 Conclusions

We studied the influence of thermal conduction on frequency response of a vaporizing droplet submitted to harmonic acoustic oscillations. As in the classical model, a mean spherical droplet, representing the spray of repetitively injected droplets in the combustion chamber allowed to evaluate the mass or heat transfer response to pressure oscillations. The idealized hypothesis of a source only concentrated at the centre of the supplied droplet was considered for two different thermal forcing types: constant temperature (isothermal injection regime) or zero temperature gradient (adiabatic injection regime). Thus, radial thermal convection effect from the centre of the droplet to its evaporating surface was neglected.

However, analytical solutions derived for mass response factor in the one hand, and in the other hand for temperature field perturbation inside the droplet permitted to determine the differences and the similarities between the two forcing regimes.

The analysis of the mass transfer response factor curves in both regimes has shown that they reach their maximum positive value at a particular reduced frequency where the lifetime of the droplet and the period of the harmonic acoustic oscillation are of the same order. But in the isothermal injection regime, this already known result [14] concerning the occurrence of the response factor peak value at a fixed frequency is valid only when the vaporization process characteristic times ratio (exchange coefficient) is inferior enough to a certain thermodynamic parameter value depending on fuel physical properties. It has been shown in the isothermal regime that, at this particular peak value frequency, by taking the characteristic times ratio inferior but closer to this parameter value, high and non-linear frequency responses may appear in the process. Once the exchange coefficient becomes superior to the thermodynamic parameter value, the response of the system diverges suddenly from the standard minimal value of -1 to much lesser negative values. Out of this particular behaviour depending on the exchange coefficient value in the isothermal feeding process, it has been shown that in both adiabatic and isothermal regimes response factor curves are quite identical for the exchange coefficient values tending to zero. Concerning the temperature field inside the mean spherical droplet, it has been seen that the perturbation due to the acoustic oscillation is significant in both regimes when the diffusion characteristic time is much lesser than the period of the harmonic acoustic disturbance. To the contrary, when the diffusion time is much greater than the period of the acoustic oscillation, the perturbation of the temperature field is negligible since the thermal wave penetration depth inside the droplet is significantly reduced regardless of the feeding process at the droplet centre. Noticeable behaviour differences between the two regimes may occur only when the diffusion time and the thermal wave period are of the same order of magnitude.

This study and its results may be relevant to the development of numerical codes for calculating two-phase flows with a consideration of thermal structures inside the droplets. The analytical solutions can serve as references to validate the codes and the physical results obtained may help to interpret the observed behaviour since the lifetime of a free vaporizing droplet can be assimilated to the injected fuel residence time for a supplied droplet. The application of the frequency response characteristics of the vaporization process to combustion chamber design may be envisioned in several ways. It is found that the residence time depends on the size of the drop, the thermal diffusion time depends on the fuel diffusivity, and the period of the oscillation can be related to the shape of the combustion chamber. A broader region of positive response implies that combustion process would be unstable for a broad range of combustion chamber designs. Thus, according to the influence of the boundary conditions controlling the vaporization process, the region of positive response and especially the magnitude of the peak response value and that of the cut-off frequency value are of primary significance in establishing systems stability limits.

This study has shown that, depending on the injection regime, fuel physical properties can have a significant effect on the frequency response of a vaporization process. As mentioned in the introduction, the reduction of the emissions of polluting gases from engines is related to the reduction of combustion instabilities. An experimental work is needed to clarify the issue since, in the isothermal centre case, the proximity of the exchange coefficient to a parameter value depending on fuel physical properties is shown to be a plausible cause for high frequency response occurrence in combustion chambers. Moreover, theoretical and experimental studies, by taking into account the often neglected thermal convection effects

inside the mean spherical droplet, need to be carried out in order to include more parameters in the instability mechanism models.

References

1. Culick, F.: Overview of Combustion Instabilities in Liquid-Propellant Rocket Engines. In: Culick, F., Yang, V. (eds.) Liquid Rocket Engine Combustion Instability, vol. 169, pp. 3-37. AIAA (1995)
2. Bhatia, R., Sirignano, W.A.: One-dimensional analysis of liquid-fuel combustion instability. Journal of Propulsion and Power 7(6), 953-961 (1991)
3. Delplanque, J.-P., Sirignano, W. A.: Transcritical liquid oxygen droplet vaporization: effect on rocket combustion instability. Atomization and sprays 4, 325-349 (1996)
4. Yang, V., Anderson, W.: Liquid propellant rocket combustion instability. Progress in Astronautics and Aeronautics, AIAA 169 (1995)
5. DiCicco, M., Buckmaster, J.: Acoustic instabilities driven by slip between a condensed phase and the gas-phase in combustion systems. 32nd AIAA Aerospace Sciences Meeting and Exhibit, Paper AIAA 94-0103, Reno, NV (USA), 10-13 (1994)
6. Dubois, I., Habiballah, M., Lecourt, R.: Numerical analysis of liquid rocket engine combustion instability. 33rd AIAA Aerospace Sciences Meeting and Exhibit, Paper AIAA-95-0607, Reno, NV (USA), 9-12 (1995)
7. Duvvur, A., Chiang, C.H., Sirignano, W.A.: Oscillatory fuel droplet vaporization: driving mechanism for combustion instability. Journal of Propulsion and Power 12(2), 358-365 (1996)
8. Harrje, D.T., Reardon, F.H.: Liquid propellant rocket combustion instability. NASA SP-194 (1972)
9. Heidmann, M.F., Wieber, P.R.: Analysis of frequency response characteristics of propellant vaporisation. NASA Technical Note D-3749 (1966)
10. Heidmann, M.F.: Frequency response of a vaporization process to distorted acoustic disturbances. NASA Technical Note D-6806 (1972)
11. Prud'homme, R.: Evaporation et combustion de gouttes dans les moteurs. Editions Techniques de l'Ingénieur, Traité de Mécanique (2009)
12. Prud'homme, R.: Flows of reactive fluids. Book Series: Fluid Mechanics and Its applications, Springer (2010)
13. Prud'homme, R., Habiballah, M., Matuszewski, L., Mauriot, Y., Nicole, A.: Theoretical analysis of dynamic response of a vaporizing droplet to acoustic oscillations. Journal of Propulsion and Power 26(1), 74-83 (2010)
14. Anani, K., Prud'homme, R., d'Almeida, S.A., Assiamoua, K.S.: Effect of thermal convection on frequency response of a perturbed vaporizing pastille-shaped droplet. Mechanics & Industry 12(4), 300-313 (2011)
15. Sazhin, S. S.: Advanced models of fuel droplet heating and evaporation. Progress in Energy and Combustion Science 32, 162-214 (2006)
16. Abramzon, B., Sirignano, W.A.: Droplet vaporization model for spray combustion calculations. Int. J. Heat Mass Transfer 32(9), 1605-1618 (1989)
17. Law, C.K.: Recent Advances in Droplet Vaporization and Combustion. Proceedings of Energy Combustion Science 8, 171-201 (1982)
18. Rayleigh, L.: The theory of sound. Macmillan (1945)
19. Sirignano, W.A., Delplanque, J.-P., Chiang, C.H., Bhatia, R.: Liquid-propellant droplet vaporization: a rate controlling process for combustion instability in Liquid rocket engine combustion instability. Edited by V. Yang, W. E. Anderson, Progress in Astronautics and Aeronautics, AIAA 169 (1994)
20. De Benedictis, M.: Instabilités couplées haute fréquence dans les moteurs-fusées ergols liquides: étude du couplage chambre de combustion / système d'alimentation. Thèse, Université de Poitiers. https://tel.archives-ouvertes.fr/tel-00283229/document (2007)
21. Mauriot, Y., Prud'homme R.: Assessment of evaporation equilibrium and stability concerning an acoustically excited drop in combustion products. C. R. Mecanique 342, 240-253 (2014)
22. Hsiao, G.C., Meng, H., Yang V.: Pressure-coupled vaporization response of n-pentane fuel droplet at subcritical and supercritical conditions. Proceedings of the Combustion Institute, 33, 19972003 (2011)
23. Lafon, P., Meng, H., Yang, V., Habiballah, M.: Pressure-coupled responses of lox droplet vaporization and combustion in high-pressure hydrogen environments. Combustion Science and Technology, 186, 11911208 (2014)
24. Lafon, P., Meng, H., Yang, V., Habiballah, M.: Vaporization of liquid oxygen (LOX)droplets in hydrogen and water environments under sub- and super-critical conditions. Combustion Science and Technology, 180, 126 (2008)